EMITTANCE DILUTION THROUGH COHERENT ENERGY SPREAD GENERATION IN BENDING SYSTEMS

P. Emma, *SLAC, Stanford, California,* USA[*]

R. Brinkmann, *DESY, 22603 Hamburg,* GERMANY

Abstract

For a bunched beam, coherent energy spread generated within a bending system may couple to the transverse (bending) plane coordinates through the chromatic transfer functions of the particular beamline—even an achromatic beamline. The resulting transverse emittance dilution is dependent on the magnitude of the energy spread, its generation rate along the beamline, and the beamline's chromatic transfer functions. The coherent energy spread may be due to resistive-wall wakefields or coherent synchrotron radiation. For specific beamlines, such as a periodic arc or wiggler, the longitudinal-to-transverse coupling is minimal and, in ideal cases, completely suppressed resulting in reduction or cancellation of all transverse emittance dilution effects. This is of particular interest for micro-bunch transport or compression systems such as exist in future FEL or linear collider projects.

1 INTRODUCTION

Many FEL and future linear collider projects utilize transport lines which bend high energy bunched electron beams—with bunch lengths in the sub-picosecond range—in order to achieve this bunch compression or, in some cases, simply to transport the micro-bunch [1,2,3]. Unfortunately, several processes exist which may generate significant energy spread as the bunch traverses this beamline, especially for a very short bunch. Along with the well known stochastic process of quantum fluctuations which produce an incoherent, random energy spread within the bunch, several mechanisms produce a coherent energy spread along the bunch such as resistive wall wakefields [4] or coherent synchrotron radiation [5,6,7].

An electron which, for example, looses energy, $\delta(s) \equiv \Delta E(s)/E_0$, at location s within this bending system will be transported to its end through the chromatic transfer functions, $\partial x/\partial \delta \equiv R_{16}(s)$ and $\partial x'/\partial \delta \equiv R_{26}(s)$, which map an off energy particle from the point of energy loss into transverse phase space at the end of the bending system. Since the energy loss can be different for different particles, the resulting energy spread can potentially dilute the transverse emittance in the bending plane depending on the coherence of the process. A random process results in an intrinsic emittance dilution which is not recoverable while a coherent energy spread generates a projected emittance dilution where correlations among the beam coordinates remain. The latter is therefore a reversible

process. We present a few idealized bending systems which, depending on the details of the coherent energy spreading process, minimize or cancel this emittance dilution. We do *not* examine the actual energy spreading processes which lead to this dilution and in most cases we use an idealized or simplified model of the process.

2 EMITTANCE DILUTION

The bend plane phase space coordinates of a particle are expressed as the vector $\mathbf{x} = [x \ x']^T$, and the rms emittance, ε, is then taken from the covariance of the particle ensemble.

$$\varepsilon^2 = \det\left\langle \mathbf{x} \cdot \mathbf{x}^T \right\rangle \quad (1)$$

As defined in the previous section, when a particle looses (or gains) energy at a location s within a bending system (even an achromatic system) its final (bending-plane) phase space coordinates at the end of the system will be altered with respect to the on-energy particle as

$$\mathbf{x}_s = \mathbf{x}_0 + \Delta\mathbf{x}(s) = \mathbf{x}_0 + \begin{bmatrix} R_{16}(s) \\ R_{26}(s) \end{bmatrix} \delta(s) \ . \quad (2)$$

(For simplicity we define coordinates such that $\langle \mathbf{x} \rangle = \langle \Delta\mathbf{x} \rangle = 0 = \langle \delta \rangle$). From Eq. (1) and (2) and an input emittance ε_0, the final emittance at bend system end is

$$\varepsilon^2 = \varepsilon_0^2 + \varepsilon_0 \left[\beta \left\langle \Delta x'^2 \right\rangle + 2\alpha \left\langle \Delta x \Delta x' \right\rangle + \gamma \left\langle \Delta x^2 \right\rangle \right] + \\ \left\langle \Delta x^2 \right\rangle \left\langle \Delta x'^2 \right\rangle - \left\langle \Delta x \Delta x' \right\rangle^2 \quad (3)$$

where β, α and γ are the nominal Twiss parameters at bend system end. The second line of Eq. (3) is an additive emittance even for a zero-emittance input beam.

For an incoherent energy loss process (i.e. δ is random with no correlation to other phase space coordinates) we first calculate the variance of $\Delta\mathbf{x}$ due to the incremental energy spread generated at each location s and sum these in quadrature over the beamline as uncorrelated quantities.

$$\left\langle \Delta x^2 \right\rangle_{\text{inc}} = \int R_{16}(s)^2 \frac{d}{ds} \sigma_\delta^2 ds \quad (4)$$

The square of the generated energy spread is represented by its rate along the beamline (similar relation for $\Delta x'$).

For a coherent process, where a particle's energy deviation is purely a function of its longitudinal position along the bunch, the transverse coordinate shifts, $\Delta\mathbf{x}(s)$, which originate at each s location add linearly, so we first sum $\Delta\mathbf{x}(s)$ over s and then find its total variance.

$$\left\langle \Delta x^2 \right\rangle_{\text{coh}} = \left(\int R_{16}(s) \frac{d\sigma_\delta}{ds} ds \right)^2 \quad (5)$$

Here the incremental energy spread generation is expressed as a rate along the beamline (similar relation for $\Delta x'$).

The difference between the incoherent and the coherent process is now clear as Eq. (4), the incoherent process, represents a monotonically increasing summation of positive values, whereas Eq. (5), the coherent process, is a summation of signed quantities which may vanish.

The full emittance dilution for the coherent process is then written from Eq. (3) where, due to coherence, the correlation $\langle \Delta x \Delta x' \rangle^2 = \langle \Delta x^2 \rangle \langle \Delta x'^2 \rangle$, and so the second line (additive emittance) is zero.

$$\varepsilon^2 \approx \varepsilon_0^2 + \varepsilon_0 \frac{1}{\beta} \left[\langle \Delta x^2 \rangle + \left(\alpha \langle \Delta x^2 \rangle^{1/2} + \beta \langle \Delta x'^2 \rangle^{1/2} \right)^2 \right] \quad (6)$$

The variances above are taken from Eq. (5). Here we assume full coherence so that, for example, a particle's energy deviation is solely a function of 1) its longitudinal position within the bunch and 2) a scalar which is equal for all particles at any particular location s along the beamline, but may vary with s (e.g. due to changing bunch length). This assumes particles do not shift with respect to each other in the bunch as will occur with a longitudinal phase space rotation of $>\pi/2$. We, therefore, only consider a functional energy dependence along the bunch whose shape does not vary significantly with s.

3 ARCS, WIGGLERS AND CHICANES

Several bending systems are of interest in future FEL and linear collider designs. We use as examples, a periodic FODO-cell arc, a simple wiggler and a magnetic chicane. There are two cases of interest for each. If we restrict ourselves to processes such as coherent synchrotron radiation (CSR) or resistive wall wakefields, which generate coherent energy spread of a magnitude which depends on the bunch length, then it is worth distinguishing between a simple transport line, where the bunch length is virtually constant, and a compressor, where the bunch length is reduced (or increased) along the beamline. We now describe how Eq.'s (5) and (6) apply to an arc, a wiggler and a chicane.

3.1 Arc

We restrict our analysis to an arc of constant bending radius constructed of FODO cells and which includes appropriate periodic dispersion matching and suppression sections prior to and following the FODO cells.

The chromatic transfer functions, $R_{16}(s)$ and $R_{26}(s)$, which map <u>from</u> locations s within an arc <u>to</u> just beyond the final dispersion suppression bend, can be shown to be periodic functions which oscillate about zero over the arc. Fig. 1 shows the dispersion function, η_x, and the transfer functions, as defined above, for a 36°-arc composed of 15 FODO cells of $\psi_x = 108°$/cell. Note, η_x maps δ (originating upstream of the first bend) to x at a location s in the arc, whereas the transfer functions map δ (originating at s) to x at a location beyond the last bend.
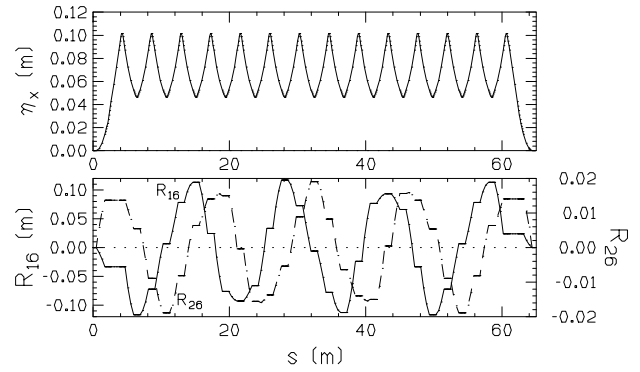
Figure 1. Dispersion function (top) and chromatic transfer functions (bot), for the example FODO-cell arc.

This arc has a 9π total phase advance and the dispersion function is matched to the periodic solution. In this case, the mean $R_{16}(s)$ and $R_{26}(s)$ are nearly zero. Therefore, a constant energy spread generation rate (e.g. constant bunch length) will generate almost no emittance increase. In Eq. (5) this implies extracting the constant energy spread rate from the integral leaving expressions for the mean R_{16} and R_{26}, both of which are nearly zero.

For a compressor-arc (changing bunch length), the energy spread generation rate must be included to evaluate the emittance growth. Fig. 2 shows the CSR emittance growth as a constant length bunch moves through the arc (a) and also for a compressing bunch (b).
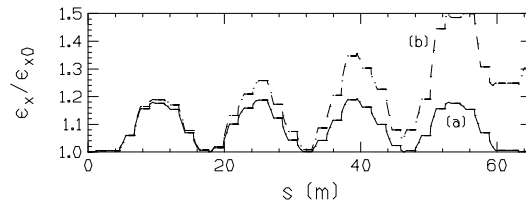
Figure 2. Fractional CSR emittance growth in arc for a constant 25-μm bunch (a) and a compressing bunch of 25-10 μm (b). The charge is 2 nC and input emittance is $\gamma\varepsilon_0 = 1$ μm.

In Fig. 2 the incremental rms coherent energy spread at each dipole magnet slice is generated as 'steady-state' CSR [7], ignoring vacuum chamber shielding, using

$$\Delta\sigma_\delta(s) \approx 0.22 \frac{r_e N \Delta L_B}{\gamma \rho^{2/3} \sigma_z^{4/3}} \quad , \quad (7)$$

where N is the bunch population, ΔL_B is the dipole magnet slice length, ρ is the bend radius, σ_z is the bunch length, r_e is the classical electron radius and γ is the Lorentz energy factor. For a constant bunch length the net arc emittance growth is zero but oscillates by up to 20%. The compressing bunch destroys the symmetry and in this case produces a net 30% growth.
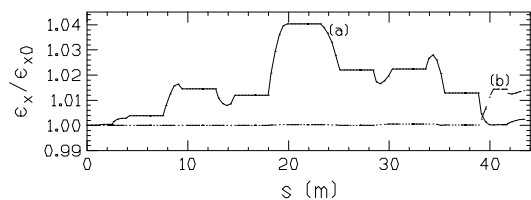
3.2 Wiggler

As an example of a wiggler system [8] we take the TESLA bunch compressor at DESY [9] which compresses a 9 mm rms bunch to 600 μm. The system is composed of eight 16° bends and two 8° bends to introduce an energy

dependent path length. The dispersion function and the transfer functions, as defined above, are shown in Fig. 3. As in the case of the arc, the transfer functions oscillate around zero.
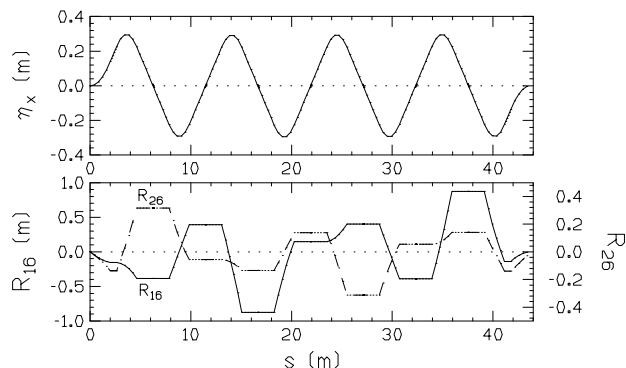
Figure 3. Dispersion function (top) and chromatic transfer functions (bot) of the TESLA bunch compressor wiggler.

The CSR emittance growth across this wiggler is shown in Fig. 4 for a 1-mm constant bunch length (a) and also a compressing bunch from 9 to 0.6 mm (b).

Figure 4. Fractional CSR emittance growth in wiggler of Fig. 3 for a constant 1-mm bunch length (a) and for a compressing bunch of 9-0.6 mm (b). The charge is 6 nC and input emittance is $\gamma \varepsilon_{x0} = 8 \mu m$.

Although the CSR effects are small, the constant bunch results in nearly full cancellation of emittance dilution whereas the compressing bunch results in a 1.5% dilution.

3.3 Chicane

As an example of a four-dipole magnetic bunch-compressor chicane we take the second compressor of the Linac Coherent Light Source (LCLS) [1] at SLAC. Its function is to compress a 390 μm rms bunch to 20 μm. This is in a regime of significant CSR and potential emittance dilution. A single 13.2-meter chicane with four 3.6°, 1.5-meter long bends can be used to make the compression but CSR calculations show the emittance more than doubles for a 1-nC beam and input emittance of 1 μm (the transfer functions do not oscillate about zero).

To compensate we form a double chicane of twice the length with separating optics (4 quadrupoles) to introduce a $-\mathbf{I}_{2 \times 2}$ bend plane transfer matrix between chicane centers. The first chicane bend angles are reduced (increasing the bunch length there which reduces the CSR energy spread) and the second chicane is set to complete the 20 μm final bunch compression such that dilution effects of the first chicane cancel with the second. The chicanes may also be empirically adjusted, if necessary, to minimize the

observed dilution while maintaining final compression. The dispersion function, bunch length (σ_{z1}=single-chicane, σ_{z2}=double-chicane) and emittance growth are shown in Fig. 5 (top-dash is η_x of the single chicane).
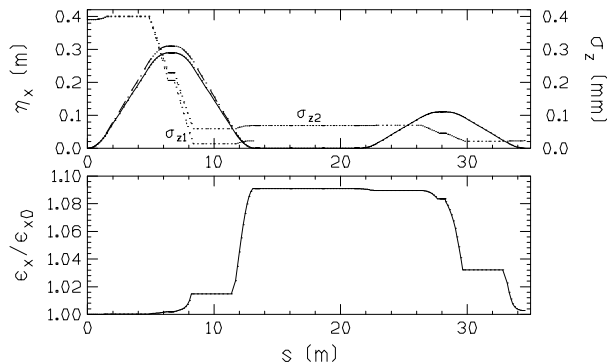
Figure 5. Dispersion (top-solid), bunch length (top-dots) and CSR emittance growth (bot) in single (σ_{z1}) and double (σ_{z2}) chicane for compressing bunch of 390-20 μm (top-dash is η_x of single chicane). The charge is 1 nC and $\gamma \varepsilon_{x0} = 1 \mu m$. Emittance growth of single-chicane ($\varepsilon/\varepsilon_0 \approx 2.3$) is not shown.

4   CONCLUSIONS

We have demonstrated that for a pure coherent energy spread generated within a bending beamline the resulting transverse emittance dilution can be minimized or canceled by a judicious choice of optics. The inherent periodicity of a FODO-cell arc and a wiggler generate cancellations which, for constant energy spread generation rate, can neutralize emittance growth. Variations on these basic bunch-compressor beamlines (e.g. the double chicane) can also be designed to compensate the emittance, even for a sharply compressing bunch. This compensation may prove useful in future FEL and linear collider projects which transport extremely short bunches.

5   REFERENCES

[1]   V.K. Bharadwaj, et al., "Linac Design for the LCLS project at SLAC", these proceedings.

[2]   "Zeroth-Order Design Report for the Next Linear Collider", SLAC Report 474, May 1996.

[3]   "Conceptual Design of a 500 GeV e^+e^- Linear Collider with Integrated X-ray Laser Facility", DESY 97-048, 1997.

[4]   O. Napoly and O. Henry, "The Resistive-Pipe Wake Potentials for Short Bunches", Part. Acc., Vol. 35, pp. 235-247, 1991.

[5]   M. Dohlus and T. Limberg, "Wake Fields of a Bunch on a General Trajectory Due to Coherent Synchrotron Radiation", these proceedings.

[6]   E.L. Saldin, et al., "On the Coherent Radiation of an Electron Bunch Moving in and Arc of a Circle", TESLA-FEL 96-14 (Nov. 1996).

[7]   Ya. S. Derbenev, et al., "Microbunch Radiative Tail-Head Interaction", DESY, Sep. 1995.

[8]   T.O. Raubenheimer, et al., "Chicane and Wiggler Based Bunch Compressors for Future Linear Colliders", SLAC-PUB-6119, May 1993.

[9]   P. Emma, "Bunch Compressor Beamlines for the TESLA and S-band Linear Colliders", DESY-TESLA 95-17 (July 1995).